Effects of adsorbate lateral repulsion on desorption and diffusion kinetics studied by Monte Carlo simulations

I. Farbman, M. Asscher, and A. Ben-Shaul

Citation: **104**, (1996); doi: 10.1063/1.471805
View online: http://dx.doi.org/10.1063/1.471805
View Table of Contents: http://aip.scitation.org/toc/jcp/104/14
Published by the American Institute of Physics

Effects of adsorbate lateral repulsion on desorption and diffusion kinetics studied by Monte Carlo simulations

I. Farbman, M. Asscher, and A. Ben-Shaul
Department of Physical Chemistry and The Fritz Haber Research Center for Molecular Dynamics, The Hebrew University, Jerusalem 91904, Israel

(Received 18 August 1995; accepted 3 January 1996)

The effects of adsorbate lateral interactions on the kinetics of surface diffusion and desorption are studied by means of kinetic and thermodynamic Monte Carlo simulations. This study is motivated by recent diffusion and desorption experiments on the NH_3/Re(001) system, which show that the activation energies of these processes decrease (in different fashions) with increasing surface coverage, the interactions between the adsorbates are thus assumed to be repulsive. A long range dipole–dipole-like potential is used to simulate both the diffusion and desorption processes. Most calculations are carried out with the interaction range extending up to fourth-order neighbors. Longer ranges are found to barely affect the kinetic behavior. On the other hand, shorter ranges of interaction result in qualitatively and quantitatively different structural (thermodynamic phase) behaviors and, consequently, in very different kinetics of diffusion and desorption. The model used to calculate diffusion kinetics assumes that the activation barrier to particle diffusion depends, simultaneously, on the local environments of both the initial and the final sites involved in the elementary event of particle jumps. The chemical diffusion coefficient is evaluated based on thermodynamic and kinetic Monte Carlo simulations. It is found to increase with surface coverage, reflecting the repulsive nature of the interactions. Yet, unlike the experimental results, the increase is nonmonotonic but rather, somewhat oscillatory—reflecting the structural phase transitions of the adsorbed layer. The activation energy of desorption is found to decrease by about 15 kcal/mole as the coverage increases from 0 to 1, showing steeper slopes around the coverages corresponding to a perfectly ordered adlayer phase. These results are in satisfactory qualitative and quantitative agreement with experiment. Finally, it is shown that the coverage dependence of the activation barrier to diffusion can be reasonably well evaluated from equilibrium thermodynamic desorption data. © *1996 American Institute of Physics.* [S0021-9606(96)00314-X]

I. INTRODUCTION

The role of lateral interactions between neighbor adsorbates in affecting the kinetics of primary surface processes has long been recognized. Adsorbate aggregation, island formation, the appearance of different overlayer structures, and phase transitions between them are among the ''mesoscopic'' manifestations of adsorbate lateral interactions. All of these phenomena affect the local environment of the adsorbed particles and are thus expected to significantly affect the kinetics of the various surface processes such as diffusion, desorption, adsorption, or chemical reaction.

Each of the above kinetic surface processes has been considered in detail separately both experimentally and theoretically.[1–5] Quite often in these studies the effects of adsorbate lateral interactions are modeled in an approximate, mean-field-like, fashion. This approach is usually accurate only in the limit of low coverage or weak interactions. In case of strong interactions, the interpretation of both theoretical and experimental (e.g., TPD) results becomes problematic. In TPD experiments uncertainty originates primarily due to the compensation effect. This effect refers to the observation that the activation energy and the preexponential factor change in the same way with coverage.[6,7] Equilibrium measurements (where both gas pressure and crystal temperature are varied) provide the best way to confront this difficulty.[8–11] However, the molecular level understanding of the results of such experiments may become ambiguous, particularly in the case of strong interactions.

These experimental difficulties inspired the development of various theoretical approaches, including Monte Carlo (MC) simulation schemes and a variety of mean-field approximations, all aiming to account for the role of coverage on the rate of desorption. These calculations have revealed that the influence of lateral adsorbate interactions are often crucial and, moreover, that, in general, they cannot be fully accounted for using simple coverage dependent rate parameters.[12–16]

In recent years experimental studies of chemical diffusion on surfaces have become more accurate and accessible for a larger variety of molecular adsorbates, due to the introduction of laser desorption and diffraction techniques.[2,17–23] These methods enable careful investigation of coverage effects on diffusion rates in systems governed by strong lateral interactions.[24–28] The recent theoretical studies of diffusion on surfaces include various lattice gas models,[12,15] MC simulations,[29–33] and mean-field calculations involving different levels of sophistication,[12,13,32] in accounting for the structural and thermodynamic effects of adsorbate lateral interactions on the chemical and tracer diffusion coefficients. Molecular dynamics simulations[34,35] have been used to treat

 0021-9606/96/104(14)/5674/9/$10.00

the dynamical aspects of diffusion and desorption.

In view of the extensive studies mentioned earlier it is rather surprising that only few theoretical studies have addressed the effects of neighbor adsorbates on these two, related, surface phenomena based on the same theoretical model.[12,36] Moreover, in most of the MC or mean-field studies the interaction potentials between neighbor adsorbates are treated as adjustable parameters, chosen to fit either structural or kinetic data. Only rarely in these studies a physical (e.g., electrostatic) model is employed to derive their functional form.[37]

In this paper we present MC simulations for a model system, attempting to scrutinize the role of adsorbate repulsive interactions on *both* the desorption and diffusion rates for a specific adsorbate-surface system. The model system attempts to explain some of the data obtained for NH_3 adsorbed on Re(001) utilizing optical second harmonic generation.[11,28,38] For this system, the isosteric heat of adsorption, the preexponential factor in the desorption rate constant and the diffusion coefficient were all determined as a function of coverage. In our theoretical treatment of this system we shall use a physically meaningful, long range dipole–dipole interaction potential, to account for the repulsive interactions between the adsorbed ammonia molecules. Adsorbate diffusion in this system has recently been investigated theoretically with the aid of a lattice gas model involving only nearest neighbor (NN) lateral interactions.[39] It is argued later that these short range interactions are probably insufficient to properly describe, not even qualitatively, the entire kinetic behavior of the experimental system.

II. MODEL

A. Energetics

We model the Re(001) surface as a perfect hexagonal lattice of adsorption sites, consistent with the assumption that the ammonia molecules adsorb uniformly at either on-top or threefold hollow sites. The exact position of the adsorption site has not been determined experimentally. The simulations were performed on two-dimensional (2D) hexagonal lattices comprising 60×60 sites, with periodic boundary conditions. Test simulations on larger lattices (84×84 sites) were performed in order to asses the importance of finite size effects, revealing that for the systems studied in this work these effects are negligible. This is consistent with the work of Sandhoff *et al.*,[40] who found a lattice of 60×60 sites to give most satisfactory results for a similar system.

Experimentally, the saturation coverage in the NH_3/Re system is $\theta_s=0.25$, indicating that the ammonia molecules cannot occupy nearest neighbor (NN) sites due to very strong (electrostatic and/or excluded volume) repulsive forces.[11] Consequently, the distance of closest approach in our simulations was set to $r_0=2$, in units of the lattice constant. Hereafter, coverages, θ, will be taken relative to the saturation coverage.

The experimental data suggest that the lateral interactions between the adsorbed ammonia molecules are repulsive.[11,28,41] We assume that they are pairwise additive and model them using a dipole–dipole interaction potential of the form:

$$U_{ij}=\begin{cases} U_0/r_{ij}^3 & \text{if } r_{ij}\leqslant r^* \\ 0 & \text{if } r_{ij}>r^* \end{cases}, \tag{1}$$

with r_{ij} denoting the distance between sites i and j, and r^* is a ''cutoff'' radius (see the following), both measured in units of r_0. The interaction potential U_0 between two adsorbates at distance r_0, was set to 2 kcal/mole in all the calculations reported later. This value corresponds, for example, to the repulsive interaction between two parallel dipoles of 2 D [the dipole moment of ammonia on Re(001) as determined by work function measurements[41]] at a distance of 3.0 Å from each other.

The cutoff distance r^* is introduced in order to keep the calculations tractable. It is supposed to represent the distance beyond which adsorbate–adsorbate interactions do not affect significantly the kinetic and structural characteristics of the adlayer. To obtain a reasonable estimate of this distance we have considered a perfectly ordered 2×2 adlayer, and, using Eq. (1), calculated the energy change ΔE associated with moving one of the adsorbed particles into a NN site (thus creating an isolated defect), as a function of r^*.

The results of this calculation are shown in Fig. 1 together with definition of the interaction ranges. Noting that ΔE does not vary significantly once $r^*/r_0\geqslant\sqrt{7}$ we have set $r^*/r_0=\sqrt{7}$ as the ''standard'' (or ''full'') interaction range in our calculations. For the sake of comparison, and for demonstrating the importance of the range of interaction in modeling surface kinetic phenomena we have also carried out some calculations for a shorter cut-off distance, namely $r^*/r_0=\sqrt{3}$. Note that $\sqrt{7}$ and $\sqrt{3}$ correspond, on the triangular lattice, to the distance between fourth-order and second-order neighbors, respectively.

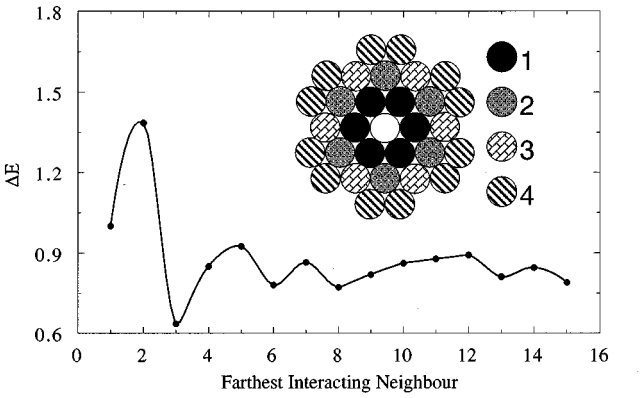

FIG. 1. The energy change, ΔE, associated with perturbing a perfect (2×2) layer by moving one particle to a nearest neighbor vacant site. The perturbation energy is shown as a function of the range r^*, of the repulsive dipole–dipole potential, see Eq. (1). For convenience the abscissa is expressed in terms of the ''farthest neighbor'' included in the range of interaction. In units of the lattice constant $r^*/r_0=1,\sqrt{3},2,\sqrt{7},...$ correspond here to farthest neighbor 1,2,3,4,..., respectively (see insert). Energy is given in units of nearest-neighbor interaction.

The model described was used to study, theoretically, the kinetics of particle diffusion and desorption as a function of coverage and temperature. The temperature range considered was 40–240 K, which includes both the temperature range of diffusion measurements (105–130 K) and equilibrium—desorption experiments (160–240 K) of the NH_3/Re system.[11,28] The diffusion and desorption experiments were modeled using Monte Carlo (MC) simulations. Additional calculations were performed based on the Bethe–Peierls approximation (BPA) for our interacting lattice gas model.

The BPA scheme has been described in detail elsewhere[12,13] and need not be repeated. Let us reiterate, however, that the basic idea in using the BPA is to focus attention on a finite ''colony'' of lattice sites. This colony is treated as an open sub system, with the rest of the system serving as a heat and matter bath. The grand-canonical partition function of the colony is then calculated by summing over the statistical weights of all possible particle configurations in the colony, taking accurately into account all interparticle interactions within the colony. Interactions between colony particles and the surroundings are treated in a mean-field fashion, assigning different effective interaction potentials to particles in different types of colony sites (e.g., edge vs center sites). Requiring that, on the average, all lattice sites should be populated with equal probabilities one then obtains self-consistency equations from which the effective (colony surroundings) potentials can be evaluated. Given these potentials one can calculate all relevant thermodynamic properties of the system.

The accuracy of the BPA calculations increases with the size of the colony, but so also the computational effort involved. Actually, above a certain colony size the MC calculations are simpler to perform than those based on the BPA. We found that for the shorter cutoff distance used ($r^*/r_0=\sqrt{3}$) the BPA calculations were both very accurate and very efficient, as compared to the MC calculations. They provided no advantage over the MC calculations once the longer cutoff distance ($r^*/r_0=\sqrt{7}$) was used.

B. Isosteric heat of adsorption

The adsorption-desorption experiments which motivated the present study were performed under equilibrium conditions.[11] Namely, the adsorbed layer has been brought to equilibrium, at different coverages and temperatures, with the molecules at the gas phase. To ensure similar conditions in our MC simulations we have first randomly populated the lattice sites according to the prescribed value of θ, and then performed particle moves, with acceptance criteria according to the usual Metropolis scheme. To enhance the equilibration process no restrictions were set on the range of particle displacements. In fact, the simulation procedure employed is equivalent to a sequence of particle desorption-adsorption events weighted, as usual, by the local interaction energies in the old and new sites.

Experimentally, the sticking coefficient of NH_3 on Re(001) is near unity and independent of coverage, implying practically zero activation energy for adsorption.[11] Consequently, the activation energy for desorption is equal to the isosteric heat of adsorption, namely,[42]

$$\Delta H = -\partial\beta\mu/\partial\beta. \tag{2}$$

Here ΔH is the adsorption enthalpy (or activation energy for desorption), μ is the chemical potential of the system, and $\beta=1/kT$, with k denoting Boltzmann's constant and T the absolute temperature.

The chemical potential was calculated, as common in canonical MC simulations, using the (Widom's) ''insertion'' formula,[43]

$$\beta\mu = \ln\,\theta - \ln[\exp(-\beta\varphi)]. \tag{3}$$

Here φ is the potential energy increment associated with the insertion of a particle into a randomly chosen lattice site (being infinite for occupied sites).

C. Diffusion kinetics

We have calculated the chemical diffusion coefficient D using the expression[4,31]

$$D = (1/4t)PC, \tag{4}$$

where t is the time, and P and C denote, respectively, the ''thermodynamic factor'' and the ''time correlation function.'' The thermodynamic factor is given by

$$P = \partial\beta\mu/\partial\,\ln\,\theta = \langle N\rangle/\langle(\delta N)^2\rangle, \tag{5}$$

where $\langle N\rangle$ is the average number of adsorbed particles and $\langle(\delta N)^2\rangle$ is the fluctuation in N.

The factor C is proportional to the time correlation function of the motion of the center of mass of the system. It is given by[4,31]

$$C = (1/N)\left\langle\left|\sum\,[r_i(t)-r_i(0)]\right|^2\right\rangle, \tag{6}$$

where $r_i(t)$ is the position of particle i at time t. The summation extends over all particles.

The derivation of Eq. (4) is discussed in detail elsewhere.[4] Qualitatively, the appearance of the thermodynamic factor in D derives from the fact that the driving force for particle diffusion are local density gradients. When the thermodynamic equilibrium state itself is characterized by large density fluctuations, this driving force decreases.

Both the thermodynamic factor and the correlation function were calculated by performing MC simulations (of different kinds, see the following) for systems in thermodynamic equilibrium. The thermodynamic factor can be calculated using either the first or the second equality in Eq. (5), namely, by calculating either $\partial\beta\mu/\partial\,\ln\,\theta$ *or* $\langle N\rangle/\langle(\delta N)^2\rangle$. The first route requires the calculation of $\beta\mu$ as a function of θ. This can be done using the particle insertion method, as mentioned with respect to Eq. (3). The second route involves grand-canonical simulations i.e., simulations at constant μ, T, and A, where A is the total area of the lattice. We have performed both types of calculations, finding generally excellent agreement between them (see Sec. III).

The correlation function C was calculated by means of kinetic MC simulations. Basically, the procedure adopted is

to follow many particle "trajectories" $r(t)$ over long periods of time and use Eq. (6) to evaluate C. The trajectories were simulated as sequences of particle jumps between nearest-neighbor sites, with transition probabilities of the Arrhenius form. More explicitly, in these simulations a particle is randomly chosen and then allowed to hop into a randomly chosen neighboring site. If the new site is already occupied the move is rejected. Otherwise it is accepted, with probability $p=\exp(-\epsilon_b/kT)$, where ϵ_b denotes the activation barrier for diffusion. As usual, one Monte Carlo step (MCS) corresponds, by definition, to one attempted move per particle (on the average). A connection between the MC time and real time is established by identifying 1 MCS$=1/\nu$, where ν is the experimental frequency of attempted jumps, which is, typically, in the range 10^{12}–10^{17} sec^{-1}. In general, ν is taken as the preexponential factor in the Arrhenius formula for the hopping rate of a single (noninteracting) particle on the surface. For the NH_3/Re system $\nu\approx 10^{15}$ sec^{-1} at $\theta=0.5$.

The activation barrier and, hence, the jump probability from one site to another depends on the local environments of both the initial and the final sites. Various expressions have been suggested to model the influence of adsorbate lateral interactions on the hopping rate [for a review see, e.g., Ref. 14(c)]. We have examined two of these models, which we have termed "the independent saddle point (ISP) scheme,"[31] and "the intersecting harmonic wells (IHW) scheme."[14(c)] These models differ in their expressions for the activation barrier. In the ISP model the barrier energy is assumed to depend only on the local environment of the initial site, i.e., on the lateral interactions of the hopping particle prior to the jump. In the IHW model ϵ_b depends on the local environments of both the initial and the final sites (see the following).

In the ISP model the activation energy for particle jump from site i to site j is only affected by interactions of the hopping particles with their neighbors in the initial site. Hence,

$$\epsilon_b(i\rightarrow j)=\epsilon_b(i)=\epsilon_b^0-V(i), \tag{7}$$

where ϵ_b^0 is the activation energy for diffusion of a noninteracting particle. The quantity $V(i)$ denotes the total interaction energy of the hopping particle with its neighbors, in the initial site. That is, $V(i)=\Sigma_k U_{ik}$. If the interactions are repulsive, as we assume in Eq. (1) then, of course, they lower the activation barrier, thus enhancing the escape rate of the particle from site i. As the coverage increases this "escaping tendency" will increase. Yet, this effect is partially compensated for by the decrease in the number of vacant neighboring sites into which the particle can jump. The actual diffusion rate will depend on the balance between these "energetic" (namely ϵ_b) and "topological" (site availability) factors.[12,14] Note that a transition rate with activation energy given by Eq. (7) satisfies, as it should, the principle of detailed balance.

To ensure, in our MC simulations, that the transition probability p does not exceed unity it is necessary to rescale the activation barrier. Namely, we use $p=\exp(-\epsilon_b'/kT)$ with $\epsilon_b'=\epsilon_b-\epsilon_{b,\min}$. Here $\epsilon_{b,\min}$ denotes the lowest possible activation energy, corresponding to the fastest process possible. In our system this amounts to a particle jumping out of a site which is fully surrounded by (repulsive) neighbors except, of course, for the vacant site onto which the jump takes place.

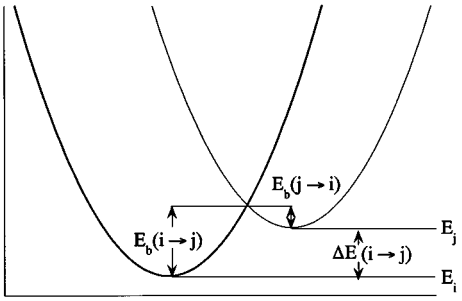

FIG. 2. A scheme of the intersecting harmonic well model for describing the diffusion barrier.

As noted earlier we have carried out kinetic MC simulations utilizing both the ISP and IHW models. The ISP model is easier to implement, yet we found that in most cases the IHW model provides better agreement with the observed experimental results. Consequently, most of the results reported in this paper were obtained using the IHW model.

In the IHW model each adsorption site is regarded as an harmonic potential well.[14] The intersection point of the potential wells corresponding to two neighboring sites i and j, is envisaged as a saddle point, see Fig. 2. The height of this saddle point, relative to the minimum of the potential well centered around site i, defines the barrier energy for the particle jump from site i to site j. The barrier height $\epsilon_b(i\rightarrow j)$ depends on the local environments of both the initial and the final sites, in a fashion specified below. It is easily verified that $\epsilon_b(i\rightarrow j)-\epsilon_b(i\rightarrow j)=\Delta\epsilon(i\rightarrow j)$ is simply the energy difference between the bottoms of the potential wells corresponding to sites j and i. Hence the model satisfies detailed balancing. The dependence of $\Delta\epsilon(i\rightarrow j)$ on the local environments of sites i and j follows from the fact that

$$\Delta\epsilon(i\rightarrow j)=V(j)-V(i), \tag{8}$$

where $V(i)$ is the quantity defined in Eq. (7).
Explicitly, the height of the activation barrier for the $i\rightarrow j$ transition is given by

$$\epsilon_b=\epsilon_b^0[1-\Delta\epsilon(i\rightarrow j)/4\epsilon_b^0]^2. \tag{9}$$

Here, as in Eq. (7), ϵ_b^0 is the barrier height for diffusion of an isolated particle or, in other words, the barrier to diffusion when $\theta\rightarrow 0$. In our calculations this quantity was taken from experiment,[28] namely $\epsilon_b^0=3.4$ kcal/mole.

III. RESULTS AND DISCUSSION

A. The role of interaction range

The range of lateral interactions plays a crucial role in determining the structure of the adsorbed layer and, hence, in the kinetics of surface processes, especially at high coverages. In Figs. 3 and 4 we demonstrate the importance of the

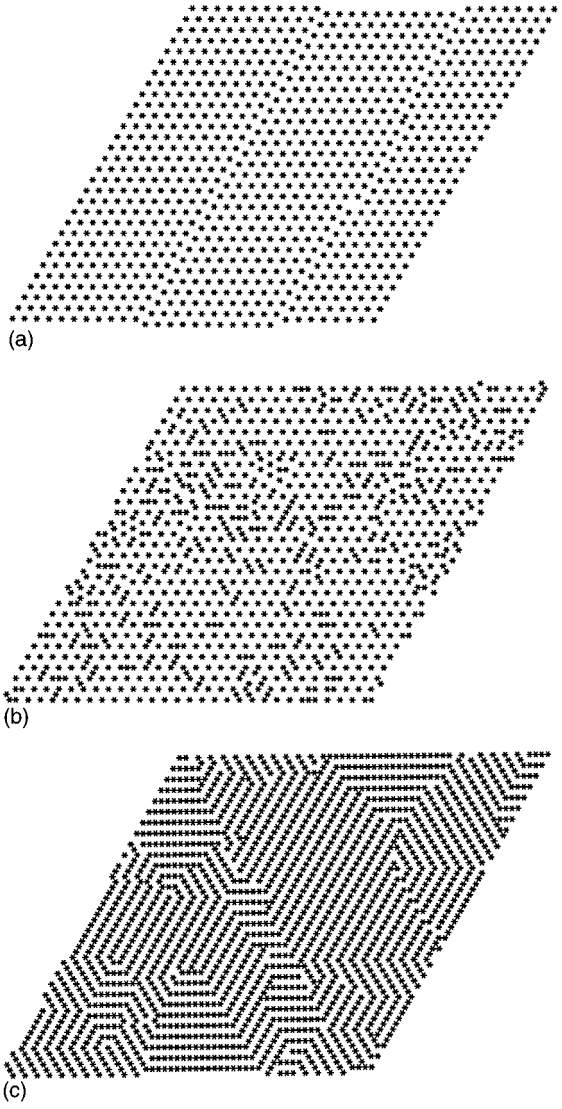

FIG. 3. Typical lattice configurations from canonical Monte Carlo simulations of a system characterized by interaction range $r^*/r_0=\sqrt{3}$. The coverages in (a), (b) and (c) are, respectively, $\theta=0.25$, 0.30, and 0.5. The temperature is 120 K.

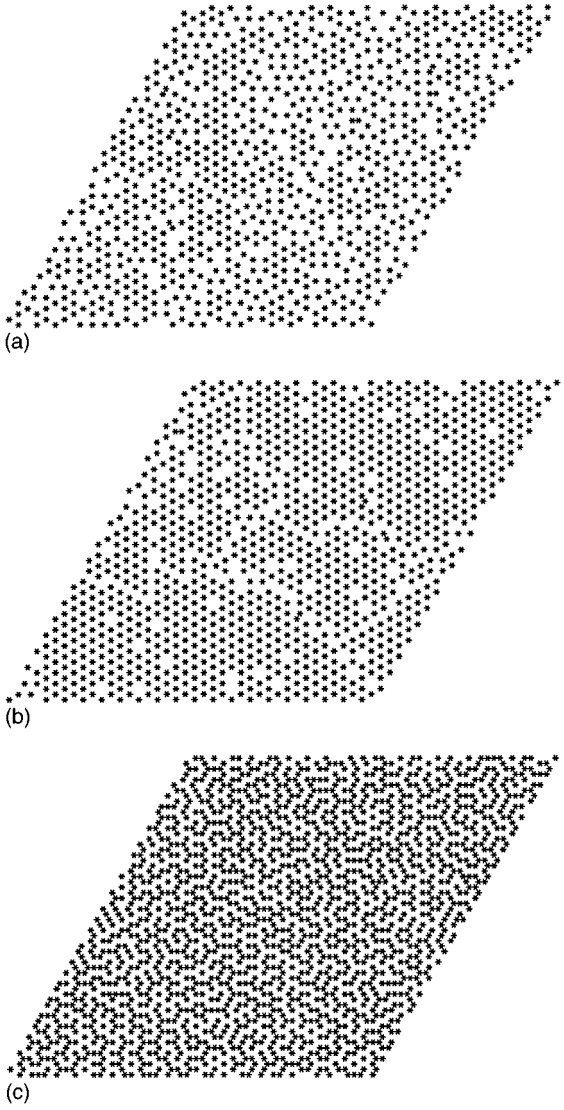

FIG. 4. Typical lattice configurations from canonical Monte Carlo simulations of a system characterized by interaction range $r^*/r_0=\sqrt{7}$. The coverages in (a), (b) and (c) are, respectively, $\theta=0.25$, 0.30, and 0.5. The temperature is 120 K.

range of interaction by showing snapshots of typical equilibrium adlayer configurations, as obtained by MC simulations based on Eq. (1), for two different choices of the cutoff distance r^*. Both Figs. 3 and 4 show configurations corresponding to coverages $\theta=0.25$, 0.30, and 0.50, all at temperature $T=120$ K. At a temperature of 240 K (the highest temperature of the equilibrium adsorption-desorption measurements) no structure is observed. In the calculations shown in Fig. 3, the interaction range is $r^*/r_0=\sqrt{3}$ (including up to second-order neighbors), while in Fig. 4 the range is $r^*/r_0=\sqrt{7}$ (including up to fourth-order neighbors). The difference between the two sets of configurations is striking. For instance, when $\theta=0.25$ the system with the shorter interaction range organizes in a perfectly ordered 2×2 overlayer [Fig. 3(a)]. This structure is no longer the one of lowest (free) energy once the interaction range increases to include third- and forth-order neighbor interactions, as indicated by the loss of long range order evidenced in Fig. 4(a).

As the coverage increases to $\theta=0.30$, the added particles in the first system adsorb randomly onto the vacant (higher energy, ''interstitial'') sites of the 2×2 adlayer, without inducing a transition to a fully disordered or a differently ordered phase, Fig. 3(b). On the other hand, in Fig. 4(b) we note the appearance of long range $\sqrt{3}\times\sqrt{3}R30°$ structure, with few isolated ''hole'' defects (which totally disappear when $\theta=1/3$). Then, when $\theta=0.5$ the system with $r^*/r_0=\sqrt{3}$ exhibits large domains of 2×1 order [Fig. 3(c)], whereas when $r^*/r_0=\sqrt{7}$, the adlayer appears as a disordered ''melt'' of short, flexible and partly branched strings of adsorbates. The latter system does not exhibit long range positional order. As the snapshots reveal, all the calculations predicted

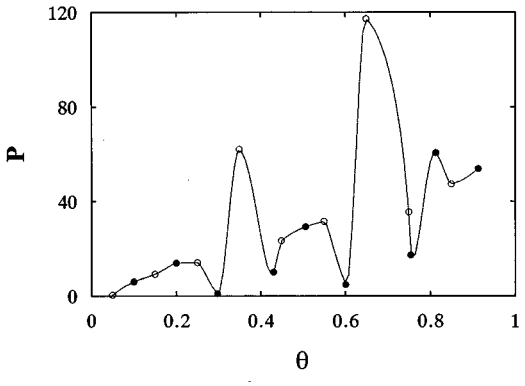

FIG. 5. Thermodynamic factor (P) as calculated by canonical (○) and grand-canonical (●) Monte Carlo simulations. In these calculations $T=120$ K and $r^*/r_0=\sqrt{7}$. The grand canonical results for $\theta=1/3$ and $\theta=2/3$ diverge.

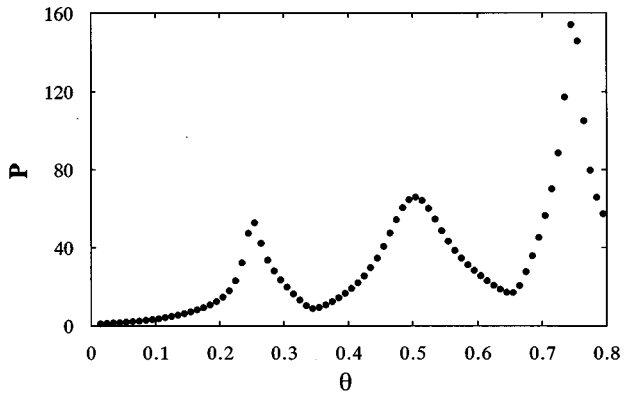

FIG. 6. Thermodynamic factor (P) as calculated using the Bethe–Peierls approximation scheme, for a system with $r^*/r_0=\sqrt{3}$, at $T=120$ K. Similar results were obtained by MC simulations.

second-order transitions (for studies of systems exhibiting first order transitions see, e.g., Ref. 44).

While it is well known that the type and range of adsorbate lateral interactions play a prominent role in determining the phase behavior of adsorbed overlayers,[40,44] the effects of these characteristics on the kinetics of surface processes has hardly been investigated. We have performed MC simulations using several different values of r^*/r_0, revealing qualitatively and quantitatively different results for both the desorption and the diffusion rates. The best (though nowhere perfect) agreement with experiment was found for the longest (''full'') range of the interaction potential ($r^*/r_0=\sqrt{7}$).

In our kinetic and thermodynamic simulations we have examined both the IHW and the ISP models described in Sec. II. According to the ISP scheme, the activation energies for desorption and diffusion are expected to show similar dependence on coverage. This follows from the fact that the barrier to diffusion in this model depends only on the initial environment of the hopping particle, which is the relevant environment affecting the rate of desorption. Our calculations show that the ISP model indeed predicts similar activation energies for diffusion and desorption. The experimental findings show both qualitative and quantitative differences between the coverage dependencies of the activation barriers of these two processes. The IHW model was found to provide a reasonable explanation of this behavior and, hence, all the (diffusion) calculations reported below are based on this model.

1. Diffusion

The diffusion coefficient D is a product of two factors, the thermodynamic factor P, and the time correlation function C, both depending sensitively on the adlayer structure. The thermodynamic factor is large whenever the fluctuations in N are small, as is the case when the system is fully ordered. In Fig. 5 the thermodynamic factor, evaluated from MC simulations, is shown as a function of the coverage, for a system with $r^*/r_0=\sqrt{7}$ at $T=120$ K. The data points in Fig. 5 were calculated using both canonical and grand-canonical simulations, revealing good agreement between the two approaches. This system, which has been considered in Fig. 4, exhibits perfect long range order when $\theta=1/3$ ($\sqrt{3}\times\sqrt{3}$) and $\theta=2/3$ ($\sqrt{3}\times\sqrt{3}$ structure of vacancies). Indeed, at $\theta=1/3$ and 2/3 the thermodynamic factor exhibits two pronounced maxima.

In Fig. 6 we show the results of MC simulations of the thermodynamic factor for a system with a shorter interaction range, $r^*/r_0=\sqrt{3}$. In this system long range order is established when $\theta=0.25,0.50,0.75$. Again, as expected, P exhibits pronounced maxima at these values of the coverage. For this system the thermodynamic factor was calculated using both the Bethe–Peierls approximation scheme, (as shown in Fig. 6) and MC simulations. The results obtained by these two approaches are in excellent agreement with each other.

At a given coverage and temperature, where D and P are constants, the time correlation function C varies linearly with time, therefore C/t is constant [see Eq. (4)]. We chose to show the coverage dependence of its time derivative (C/t) as presented in Fig. 7 for the system with the longer interaction range at $T=120$ K. Here we find that C/t obtains minima at those coverages (of perfect long range order) where the thermodynamic factor is maximal. Not surprisingly, the diffusion coefficient, D, which is a product of P and C/t varies sen-

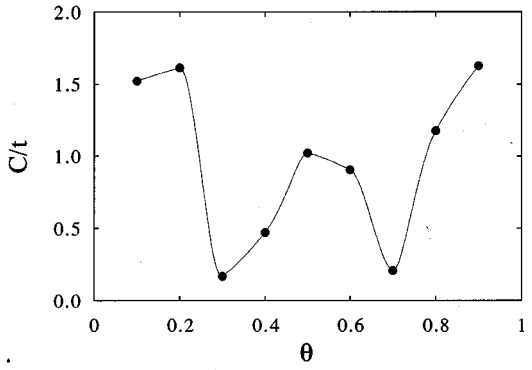

FIG. 7. The time derivative of the correlation function (C/t) as a function of coverage.

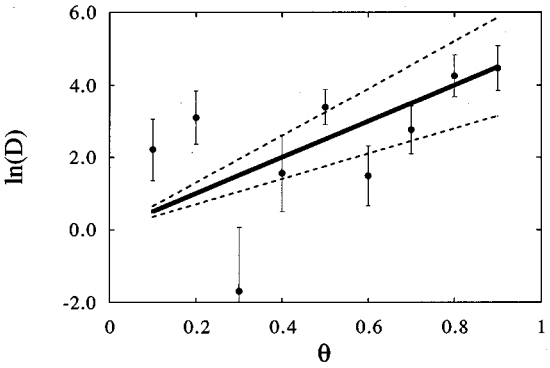

FIG. 8. The chemical diffusion coefficient D as a function of coverage, at $T=120$ K. The experimental results (Refs. 11 and 28) are shown as heavy solid line, with the dashed lines marking the uncertainty limits. The dots are the results of MC simulations ($r^*/r_0=\sqrt{7}$).

sitively, seemingly erratically, with θ, as shown in Fig. 8. Notwithstanding the (considerable) computational errors, we note that D is not a smooth function of θ, reflecting the transitions undergone by the adlayer between phases of different symmetries. Experimentally, due perhaps to kinetic effects (activation and nucleation barriers to phase transitions, and the appearance of defects in and between the finite size domains of ordered structures), the diffusion coefficient varies more smoothly with coverage (see the following).

2. Desorption

Whenever the adlayer is fully ordered any addition of particles into vacant ''interstitial'' sites involves the creation of high energy defects. For instance, adding particles to the perfectly ordered ($\sqrt{3}\times\sqrt{3}$) layer of the $r^*/r_0=\sqrt{7}$ system, results in the formation of several high energy NN contacts. Particle desorption from these (''defect'') sites is easier than desorption from the ordered phase and we expect a change in the slope of the activation energy for desorption around $\theta=1/3$. Just above $\theta=1/3$, the added particles can adsorb far apart from each other (even when randomly distributed among the available sites) thus avoiding repulsive interactions between them. At this coverage range we expect the desorption rate to change (decrease) rather slowly, since the desorbing particles are those adsorbed at the interstitial sites. The decrease of the activation energy for desorption with coverage is due to lateral interactions between these interstitial adsorbates. Eventually another ordered phase will appear (e.g., the $\sqrt{3}\times\sqrt{3}$ structure of vacancies at $\theta=2/3$) and the activation energy will again exhibit a sharp change with coverage. These qualitative trends are corroborated both experimentally and theoretically, as discussed next.

B. Comparison with experiment

The coverage dependence of the activation energy for desorption, as obtained experimentally for the NH_3/Re(001) system, is shown in Fig. 9. Also shown in Fig. 9 are the results of our MC simulations. Both the experimental and the theoretical results show marked changes in slope at two intermediate coverages. In the simulations these changes take place at $\theta=1/3$ and 2/3, consistent with the qualitative analysis already mentioned. The experimental changes in slope occur at $\theta\approx 0.3$ and 0.75. Considering the complexity of the system investigated and the high sensitivity of the desorption rate to phase changes, as demonstrated in previous sections, we regard the comparison between theory and experiment as satisfactory. The quantitative agreement, at least with regards to the range of variation of the activation energy is also reasonable. It should be added that the uncertainties in the experimental values corresponding to the limits of low and high coverage are considerable (± 2 kcal/mole).

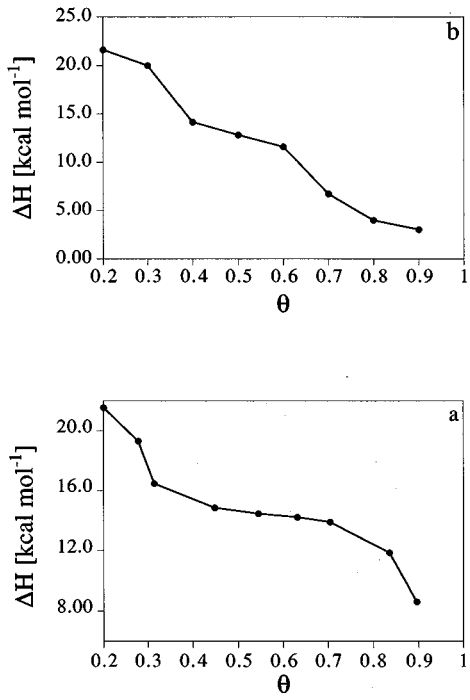

FIG. 9. Activation energy for desorption: (a) Experimental results; (b) Monte Carlo simulations.

In Fig. 8, where we showed the calculated diffusion coefficient, we also show the $D(\theta)$ curve obtained experimentally for the NH_3/Re(001) system. The simulations involve considerable uncertainties due, mainly, to difficulties associated with the calculation of the correlation function C. These are reflected by the large error bars associated with the theoretical points in Fig. 8. The experiments also involve sizable uncertainties (± 1 in $\ln\{D\}$, which originates from ± 0.2 kcal/mole in activation energy), associated with the interpretation of the grating-diffusion measurements. Considering all these provisos, the agreement between experiment and theory shown in Fig. 8 should be regarded as reasonable.

In judging the agreement between experiment and theory it should be noted that we have used the same model, namely Eq. (1), to describe both the desorption and the diffusion experiments. The strength of the dipole–dipole-like interaction potential was chosen to fit the desorption data, but no further adjustments were made to fit the diffusion measurements.

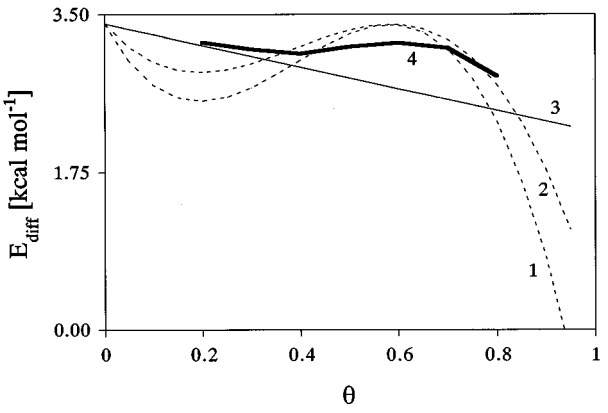

FIG. 10. Coverage dependence of the activation energy for diffusion, calculated according to Eq. (10), using thermodynamic data. Curve 1: Isosteric heat of adsorption measurements, at 190 K. Curve 2: Isosteric heat of adsorption measurements, at 160 K. Curve 3: Best fit to experimental diffusion data in the temperature range $T=110-135$ K. Curve 4: Monte Carlo simulations at $T=120$ K.

C. Theoretical analysis

We conclude the discussion by comparing our experimental and theoretical results to the predictions of the theory of diffusion developed by Reed and Ehrlich.[32] According to this theory the activation energy for diffusion can be written as

$$\epsilon_b = \epsilon_b^* + (1/P)\partial \Delta H/\partial \theta, \tag{10}$$

where $\epsilon_b(\theta)$ the activation energy for diffusion and ϵ_b^* denoting the jump activation energy for an adparticle. ϵ_b^* is coverage and temperature dependent. Equation (10) relates, therefore, a kinetic characteristic of the system, ϵ_b, to thermodynamic properties such as the thermodynamic factor, P, and the heat of adsorption ΔH. In principle, Eq. (10) enables the extraction of the microscopic jump activation energy (ϵ_b^*) from the macroscopic quantities mentioned above.

Experimentally it is impossible to conduct both adsorption-desorption and diffusion measurements at the same temperature range. Yet, in Ref. 45 it was shown that when the thermodynamic properties appearing in Eq. (10) are taken from desorption experiments (and extrapolated to the relevant temperature range) this formula accounts reasonably well for the measured diffusion coefficients. We have carried out a similar analysis based on our MC simulations. The results are summarized in Fig. 10. Three of the curves in this figure show the activation energy for diffusion, evaluated using Eq. 10, with the relevant thermodynamic quantities derived from independent equilibrium-thermodynamic measurements.[11] The jump activation energy was taken as independent of temperature and coverage, thus enables the demonstration of these dependencies as the difference between the experimental result (curve 3 in Fig. 10) and the calculated one (curve 4 in Fig. 10). The last curve is obtained when we use our equilibrium MC simulations to evaluate the second term on the right-hand side of Eq. (10). Again, considering the complex phase behavior of the simulated system we regard the agreement between the kinetically computed diffusion coefficient and the one derived "thermodynamically" based on Eq. (10) as satisfactory.

IV. CONCLUDING REMARKS

We have demonstrated that the dependencies on coverage of the activation energies corresponding to two very different surface processes—desorption and diffusion—can be explained using one rather simple theoretical model. The basic assumption of the model is that the lateral interactions between the adsorbed particles are repulsive and can be modeled using a dipole–dipole-like interaction potential, with a rather long range of interaction.

We found that a kinetic model to diffusion in which the activation barrier depends on lateral interactions of the hopping particles in both the initial and final sites provides better agreement with experiment, as compared to a model in which the hopping rate depends only on the local environment of the initial site. The coverage dependencies of the activation energy for desorption, the thermodynamic factor, and the correlation function were all found to depend critically on the range of interaction. We found that a reasonable fit to the experimental data is obtained by setting the repulsion between nearest neighbors at 2 kcal/mole. This value is 5.7 times larger than the repulsion between two ammonia dipoles at the minimum separation [assumed to be dictated by a (2×2) structure].[41] This discrepancy has not been analyzed within the framework of this work.

However, in an independent theoretical study the structure and interaction of ammonia on Pt(111) has been investigated.[46] In this study, LDA theory was employed to calculate the interaction of NH_3 molecules with a slab of 91 Pt atoms in three layers. Due to the exceptionally large size of the slab used in this computation, lateral interactions could be calculated as a function of separation distance between neighbor ammonia molecules. The repulsion between neighbors up to the fifth-order was found to decrease almost perfectly as $1/r^3$, with the interaction energy of 0.086 eV (2.0 kcal/mole) at a distance of 5.48 Å. This is the distance between two ammonia molecules adsorbed at a structure of 2×2 on the Pt(111) surface. Although in our system the metal surface is Re(001), the distance of closest approach of the ammonia molecules in a 2×2 structure is identical to that on Pt(111). In addition, work function of ammonia on Pt(111) was measured to be 2.1 eV at saturation coverage also identical to that measured on Re(001). This similarity in the behavior of ammonia on Pt(111) and on Re(001) implies that the calculations described above for Pt(111) may be valid for Re(001) as well.

V. ACKNOWLEDGMENTS

We wish to thank D. R. Jennison for providing his results prior to publication. This work was partially supported by a grant from the Israel Science Foundation and by the US–Israel Binational Science Foundation. The Fritz Haber Research Center is supported by the Minerva Gesellschaft für die Forschung, mbH, Munich, BRD.

[1] D. P. Woodruff and T. A. Delchar, *Modern Techniques of Surface Science*, 2nd Ed. (Cambridge University Press, Cambridge, 1994).
[2] J. T. Yates, Jr., in *Methods of Experimental Physics*, Vol. 32 of *Solid State Physics-Surfaces*, edited by R. L. Park and M. G. Lagally (Academic, New York, 1985), Chap. 8.
[3] G. Ehrlich and K. Stolt, Ann. Rev. Phys. Chem. **31**, 603 (1980).
[4] R. Gomer, Rep. Prog. Phys. **53**, 917 (1990).
[5] J. K. Norskov, S. Holloway, and N. D. Lang, J. Vac. sci. Technol. A **3(3)**, 1668 (1985).
[6] P. J. Estrup, E. F. Greene, M. J. Cardillo, and J. C. Tully, J. Phys. Chem. **90**, 4099 (1986).
[7] J. L. Taylor and W. H. Weinberg, Surf. Sci. **78**, 259 (1978).
[8] E. G. Seebauer, A. C. F. Kong, and L. D. Schmidt, Surf. Sci. **176**, 134 (1986).
[9] M. Chelvayohan and R. Gomer, Surf. Sci. **186**, 412 (1987).
[10] H. Pfnür and D. Menzel, J. Chem. Phys. **79**, 2400 (1983).
[11] Z. Rosenzweig and M. Asscher, Surf. Sci. **225**, 249 (1990).
[12] M. Silverberg and A. Ben-Shaul, J. Chem. Phys. **87**, 3178 (1987); Surf. Sci. **214**, 17 (1989).
[13] D. L. Adams, Surf. Sci. **42**, 12 (1974).
[14] (a) E. S. Hood, B. H. Toby, and W. H. Weinberg, Phys. Rev. Lett. **55**, 2437 (1985); (b) H. C. Kang and W. H. Weinberg, Surf. Sci. **299/300**, 755 (1994); (c) H. C. Kang and W. H. Weinberg, Acc. Chem. Res. **25**, 253 (1992).
[15] V. P. Zhdanov, Surf. Sci. **137**, 515 (1984).
[16] O. M. Becker, I. Chacham, M. Asscher, and A. Ben-Shaul, J. Phys. Chem. **93**, 8059 (1989).
[17] S. M. George, A. M. DeSantolo, and R. B. Hall, Surf. Sci. **159**, L425 (1985).
[18] C. H. Mak, J. L. Brand, A. A. Deckert, and S. M. George, J. Chem. Phys. **85**, 1676 (1986).
[19] E. G. Seebauer and L. D. Schmidt, Chem. Phys. Lett. **123**, 129 (1985).
[20] X. D. Zhu, Th. Rasing, and Y. R. Shen, Phys. Rev. Lett. **61**, 2883 (1988).
[21] T. Suzuki and T. F. Heinz, Opt. Lett. **14**, 1201 (1989).
[22] X. D. Zhu, A. Lee, and A. Wong, Appl. Phys. A **52**, 317 (1991).
[23] Xu-Dong Xiao, Yuanlin Xie, and Y. R. Shen, Surf. Sci. **271**, 295 (1992).
[24] A. A. Deckert, J. L. Brand, M. V. Arena, and S. M. George, Surf. Sci. **208**, 441 (1989).
[25] Xu-Dong Xiao, X. D. Zhu, W. Daum, and Y. R. Shen, Phys. Rev. B **46**, 9732 (1992); *ibid*. **48**, 17 452 (1993).
[26] G. A. Reider, U. Hofer, and T. F. Heinz, Phys. Rev. Lett. **66**, 1994 (1991).
[27] X. D. Zhu, A. Lee, A. Wong, and U. Linke, Phys. Rev. Lett. **68**, 1862 (1992).
[28] Z. Rosenzweig, I. Farbman, and M. Asscher, J. Chem. Phys. **98**, 8277 (1993).
[29] M. Bowker and D. A. King, Surf. Sci. **71**, 583 (1978); *ibid*. **72**, 208 (1978).
[30] M. C. Tringides and R. Gomer, Surf. Sci. **265**, 283 (1992).
[31] C. Uebing and R. Gomer, J. Chem. Phys. **95**, 7626 (1991).
[32] D. A. Reed and G. Ehrlich, Surf. Sci. **102**, 588 (1981).
[33] S.-L. Lee, F.-Y. Li, and C. Li, Chem. Phys. Lett. **168**, 283 (1990).
[34] Y. Zeiri, A. Redondo, and W. A. Goddard III, Surf. Sci. **131**, 221 (1983).
[35] K. D. Dobbs and D. J. Doren, J. Chem. Phys. **99**, 10041 (1993).
[36] B. Terreault, J. Appl. Phys. **62**, 152 (1987).
[37] J. K. Norskov, in *The Chemical Physics of Solid Surfaces and Heterogeneous Catalysis*, edited by D. A. King and D. P. Woodruff (Elsevier, Amsterdam, 1992), Vol. 6.
[38] Z. Rosenzweig and M. Asscher, J. Chem. Phys. **96**, 4040 (1992).
[39] A. Danani, R. Ferrando, E. Scalas, M. Torri, and G. P. Brivio, Chem. Phys. Lett. **236**, 533 (1995).
[40] M. Sandhoff, H. Pfnür, and H.-U. Everts, Surf. Sci. **280**, 185 (1993).
[41] M. Asscher, Proc. SPIE-Int. Soc. Opt. Eng. **2125**, 19 (1994).
[42] S. H. Payne and H. J. Kreuzer Surf. Sci. Lett. **259**, L781 (1991).
[43] M. P. Allen and D. J. Tildesley in *Computer Simulation of Liquids*, (Oxford Science Publications, Oxford, 1992), pp. 49–50.
[44] J. S. Walker and M. Schick, Phys. Rev. B **20**, 2088 (1979); K. A. Fichthorn, E. Gulari, and R. M. Ziff, Surf. Sci. **243**, 273, (1991); P. Piercy, K. De'Bell, and H. Pfnür, Phys. Rev. B **54**, 1869 (1992); M. Sandhoff, H. Pfnür, and H.-U. Everts, Europhys. Lett. **25**, 105 (1994).
[45] I. Farbman, Z. Rosenzweig, and M. Asscher, J. Chem. Soc. Faraday Discuss. **96**, 307 (1993).
[46] D. R. Jennison, P. A. Schultz, and M. P. Sears, Surf. Sci. (submitted).